

Conformational and Optical Characteristics of Unidirectionally Twisted Binaphthyl-Bipyridyl Cyclic Dyads

Kazuto Takaishi,^{*,†,‡,§} Jun Suzuki,[†] Tatsuya Yabe,[†] Hikaru Asano,[†] Michihiro Nishikawa,[†] Daisuke Hashizume,[§] Atsuya Muranaka,[‡] Masanobu Uchiyama,^{‡,||} and Akihiro Yokoyama^{*,†}

[†]Faculty of Science and Technology, Seikei University, Musashino, Tokyo 180-8633, Japan

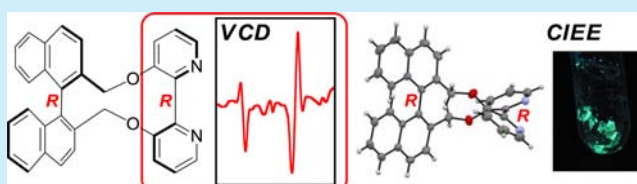
[‡]Elements Chemistry Laboratory, RIKEN, and Advanced Elements Chemistry Research Team, RIKEN, Center for Sustainable Resource Science (CSRS), Wako, 351-0198, Japan

[§]Materials Characterization Support Unit, RIKEN Center for Emergent Matter Science (CEMS), Wako 351-0198, Japan

^{||}Graduate School of Pharmaceutical Sciences, The University of Tokyo, Tokyo 113-0033, Japan

S Supporting Information

ABSTRACT: An axially chiral binaphthyl-bipyridyl cyclic dyad in which the two units are connected by short $-\text{CH}_2\text{O}-$ linkers was synthesized. Experimental and theoretical analyses indicate that the (*R*)-binaphthyl unit in the dyad induces (*R*)-chirality in the bipyridyl unit, both in the solid state and in solution. It is shown that vibrational circular dichroism (VCD) is useful to determine the twisting pattern of 2,2'-bipyridyl compounds. The dyad shows crystallization-induced emission enhancement (CIEE).



2,2'-Bipyridyl compounds are frequently used as ligands, motifs in supramolecular architectures, and components of optical materials.¹ Although 2,2'-bipyridyl derivatives with stereocenters on the side chains have been reported as ligands of catalytic asymmetric reactions,^{1c,2} there have been few studies on construction of unidirectionally twisted bipyridyl itself because bipyridyl, especially the *N*-unsubstituted charge-free bipyridyl, can rotate freely about its axis.³ Conformationally stable axially chiral bipyridyl has great potential for construction of chiral materials, so a simple synthetic approach to chiral bipyridyl scaffolds and a versatile method to determine the twisting direction of bipyridyl are required. In our previous study on axially chiral binaphthyl-azobenzene cyclic dyads, we found that the chiral axis of binaphthyl induces helicity of (*Z*)-azobenzene and planar chirality of (*E*)-azobenzene via intramolecular chiral transfer.⁴

In the present work, we designed axially chiral binaphthyl-bipyridyl cyclic dyad **1** (Figure 1) on the assumption that (1) axial chirality of the conformationally stabilized bipyridyl unit would be induced by the established axial chirality of the binaphthyl unit due to the use of short $-\text{CH}_2\text{O}-$ linkers, (2) the restriction on conformational change owing to the relatively tight structure would result in new optical properties, and (3) the small symmetrical unit of the binaphthyl-bipyridyl cyclic dyad would make it easy to elucidate its conformation and properties, and their relationships. This paper describes the synthesis, conformational analyses, and optical properties of **1** and its partial components **2**, **3**, biphenyl analogue **4**, and regioisomer **5** as reference compounds. The configurations (or conformations) of binaphthyl, bipyridyl, and biphenyl are labeled as $R_{\text{nap}}/S_{\text{nap}}$, $R_{\text{py}}/S_{\text{py}}$, and $R_{\text{ph}}/S_{\text{ph}}$, respectively.

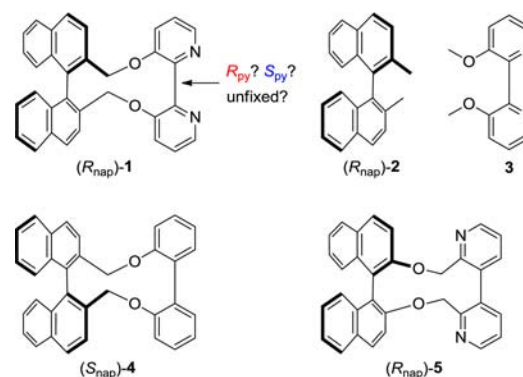
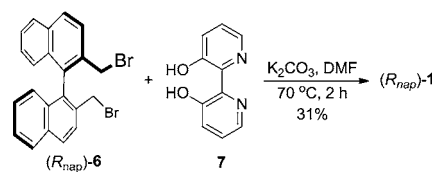


Figure 1. Structures of (R_{nap})-1 and reference compounds 2–5.

Cyclic dyad (R_{nap})-1 was synthesized in moderate yield by coupling equimolar amounts of 2,2'-bis(bromomethyl)-binaphthyl ((R_{nap})-6)⁵ and 3,3'-dihydroxy-2,2'-bipyridyl (**7**),⁶ accompanied by several cyclic and acyclic oligomers (Scheme 1).

Scheme 1. Synthesis of (R_{nap})-1



Received: July 16, 2015

Published: August 11, 2015

(R_{nap})-1 was purified easily by means of GPC. (S_{nap})-1 was also synthesized from (S_{nap})-6 and 7. Compound 3 was synthesized as reported by Teicco.⁷ (S_{nap})-4 and (R_{nap})-5 were similarly synthesized, as described in the Supporting Information.

We initially focused on the twist direction and angle of the two pyridine rings of 1. DFT calculations at the B3LYP/6-311++G(d,p) level were used to predict the conformation of the bipyridyl moiety and θ_{py} (N–C–C–N) of (R_{nap})-1.⁸ Two stable conformations were found: the ($R_{\text{nap}}, R_{\text{py}}$)-form ($\theta_{\text{py}} = -56.1^\circ$) as the most stable structure, and the ($R_{\text{nap}}, S_{\text{py}}$)-form ($\theta_{\text{py}} = +55.8^\circ$) as the second most stable structure, which is less stable by 5.5 kcal/mol (Figure 2a). That is, the theoretical calculations predict

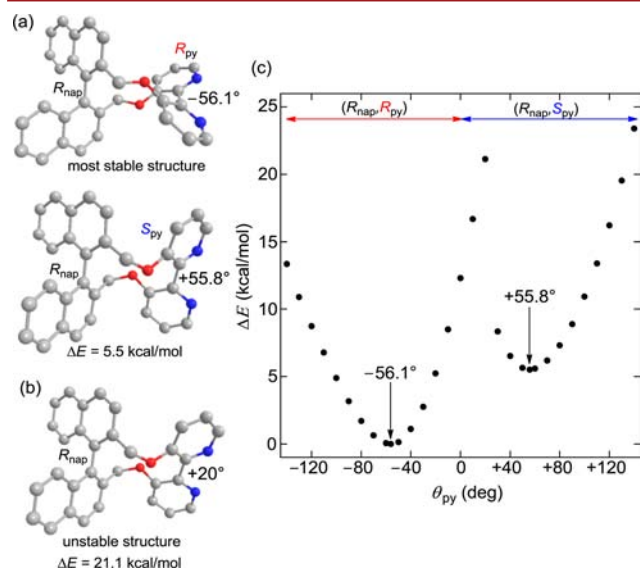


Figure 2. (a) Two stable structures of (R_{nap})-1. (b) Unstable structure of (R_{nap})-1. (c) Relationship between the energy difference and bipyridyl dihedral angle of (R_{nap})-1. θ_{py} is the dihedral angle of N–C–C–N. Calculations were carried out at the B3LYP/6-311++G(d,p) level in the gas phase. Gray, blue, and red indicate carbon, nitrogen, and oxygen, respectively. Hydrogen atoms are not shown.

that, in (R_{nap})-1, the R_{py} conformation of the bipyridyl unit is more stable than the S_{py} one. We also examined the relationship between θ_{py} in 10° increments and the energy difference at the same calculation level (Figure 2c). According to the energy profile, θ_{py} of the most unstable structure is $+20^\circ$ and its ΔE is 21.1 kcal/mol (this structure is not the transition state). In the unstable structure, the oxygen atom and the connected pyridine ring cannot be arranged in the same plane ($\angle\text{N–C–C–O} = 163.3^\circ$) due to the restriction imposed by the $-\text{CH}_2\text{O}-$ spacer (Figure 2b). These results indicate that the isomerization barrier of the bipyridyl moiety is sufficiently high to prevent isomerization from the ($R_{\text{nap}}, R_{\text{py}}$)-form to the ($R_{\text{nap}}, S_{\text{py}}$)-form, at least under normal conditions.⁹ The ($R_{\text{nap}}, R_{\text{py}}$)-form is predicted to have a value of the isomerization barrier close to that of Jaime's rigid butylene-bridged bipyridyl (isomerization barrier = 21.2 kcal/mol)¹⁰ and Rebek's bipyridyl crown ether (isomerization barrier = 25.7 kcal/mol).¹¹ Regardless of whether or not isomerization occurs, the ($R_{\text{nap}}, R_{\text{py}}$)-form is likely the preferred structure. Calculations at the B3LYP/6-31G(d,p), M06-2X/6-31G(d,p), and B97D/TZVP levels yielded similar conclusions to the calculation at the B3LYP/6-311++G(d,p) level (Figures S7–S9).

To determine the conformation of (R_{nap})-1 by X-ray crystallographic analysis, single crystals were prepared. We

obtained three kinds of crystals: (R_{nap})-1 containing chloroform ($\theta_{\text{py}} = -49.7^\circ$, Figure 3), $1/2(\text{MeOH})\cdot\text{H}_2\text{O}$ ($\theta_{\text{py}} = -49.4^\circ$,

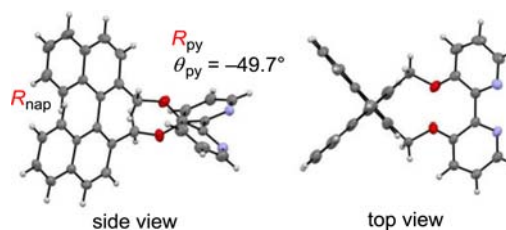


Figure 3. Single-crystal X-ray structure of (R_{nap})-1·CHCl₃. θ_{py} is the dihedral angle of N–C–C–N. Gray, white, blue, and red indicate carbon, hydrogen, nitrogen, and oxygen, respectively. The CHCl₃ molecule was omitted for clarity. Thermal ellipsoids are drawn at the 50% probability level.

Figure S1), and $1/3(\text{H}_2\text{O})$ ($\theta_{\text{py}} = -53.1^\circ$, Figure S2). In all cases, the conformation of the bipyridyl moiety is R_{py} , in which the θ_{py} values are almost the same as one another and are similar to the computationally optimized value. At present, the effects of the solvent molecules are unknown.

Next, we examined the conformation and rigidity of (R_{nap})-1 in solution, since the stable conformation in solution may differ from the crystal structure. Determination of the conformation of the chiral axis of the bipyridyl moiety from ECD spectra is difficult, because most of the UV–vis absorption region of bipyridyl overlaps with that of binaphthyl. Moreover, the intensity of the ECD signals of binaphthyl compounds is strong and sensitive to small changes of the dihedral angle between the two naphthalene rings.¹² Consequently, the ECD spectrum of (R_{nap})-1 is strongly affected not by the bipyridyl moiety, but by the binaphthyl moiety (ECD and UV–vis spectra of (R_{nap})-1, (R_{nap})-2, and 3 are shown in Figure S11). To gain information regarding the axial chirality of the bipyridyl moiety independently of that of the binaphthyl moiety, we measured the vibrational circular dichroism (VCD) spectra (Figure 4a).¹³ Two “bipyridyl regions” can be distinguished: $1600\text{--}1550\text{ cm}^{-1}$ (C–C and C–N stretch of pyridine ring) and $1480\text{--}1430\text{ cm}^{-1}$ (C–H in-plane deformation of pyridine ring).¹⁴ In these regions, theoretically optimized ($R_{\text{nap}}, R_{\text{py}}$)-1 and ($R_{\text{nap}}, S_{\text{py}}$)-1 display

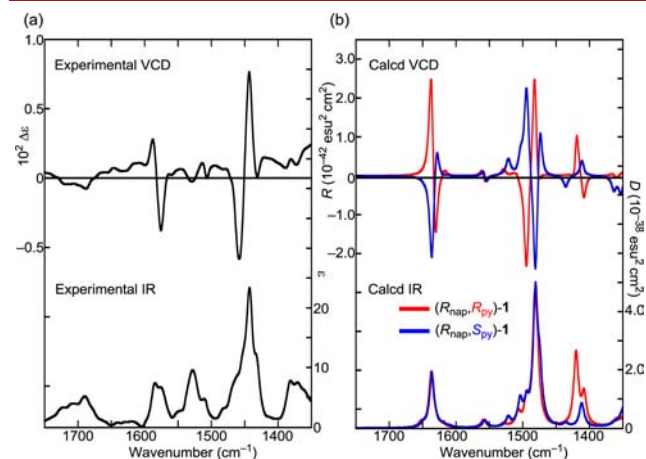


Figure 4. (a) Experimental VCD and IR spectra of (R_{nap})-1 (CDCl₃, 0.10 M, 20 °C, light path length = 0.15 cm, BaF₂). (b) Calculated VCD and IR spectra of optimized ($R_{\text{nap}}, R_{\text{py}}$)-1 (red) and ($R_{\text{nap}}, S_{\text{py}}$)-1 (blue) at the B3LYP/6-311++G(d,p) level. Half-width at half height = 4 cm⁻¹.

mirror-image split signals (Figure 4b). The experimentally observed VCD spectrum of (R_{nap})-1 agrees well with that of the ($R_{\text{nap}},R_{\text{py}}$)-form, while enantiomeric (S_{nap})-1 exhibits a mirror image of the VCD spectrum of (R_{nap})-1 along the abscissa (Figure S12). These results indicate that the inherently preferred conformation of (R_{nap})-1 is the ($R_{\text{nap}},R_{\text{py}}$)-form both in the solid state and in solution. Additionally, the relationship between the twisting patterns of 3 and the VCD signals in the larger wavenumber region was theoretically investigated (Figure 5).

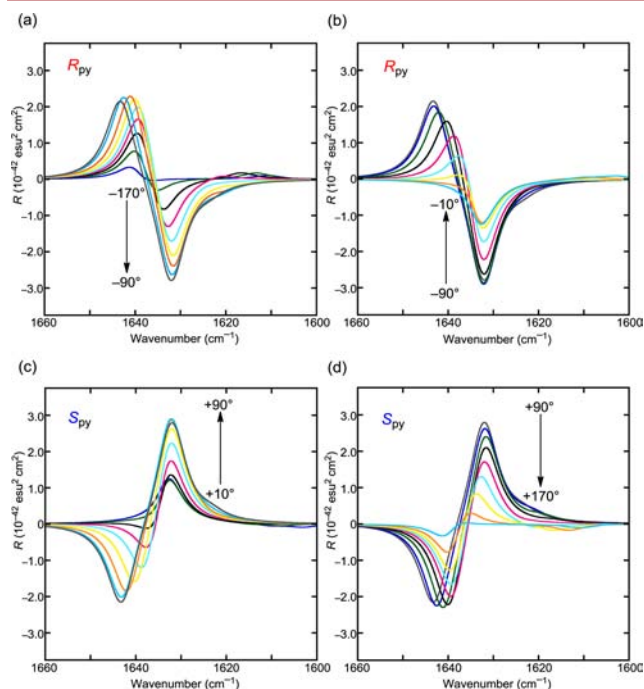


Figure 5. Relationship between the theoretical VCD spectra and the dihedral angles θ_{py} ($\angle\text{N}-\text{C}-\text{C}-\text{N}$) in 10° increments of optimized 3 at the B3LYP/6-31G(d,p) level from (a) -170° to -90° ((R_{py}) -form), (b) -90° to -10° ((R_{py}) -form), (c) 10° to 90° ((S_{py}) -form), and (d) 90° to 170° ((S_{py}) -form). Half-width at half height = 4 cm^{-1} .

(R_{py})-3 shows a negative split VCD (Figure 5a and 5b), whereas (S_{py})-3 shows a positive split VCD (Figures 5c and 5d). The positive and negative signs are abruptly exchanged at θ_{py} values of 0° and 180° . We consider VCD has the potential to become a standard method to determine the absolute conformation (or configuration) of axially chiral bipyridyls.¹⁵

To view the isomerization from ($R_{\text{nap}},R_{\text{py}}$)-1 to ($R_{\text{nap}},S_{\text{py}}$)-1, variable-temperature (VT) ^1H NMR spectra of (R_{nap})-1 were obtained in the range of -50 – 150°C , but coalescence, major changes in the chemical shifts, and signal sharpness were not observed (Figure S16). The spectrum at rt was nearly independent of solvent (CDCl_3 , CD_3OD , $\text{DMSO}-d_6$) and concentration (0.01–0.1 M) (Figures S16 and S17). These results indicate that ($R_{\text{nap}},R_{\text{py}}$)-1 is rigid, and neither marked epimerization of the bipyridyl axis nor aggregation occurs under the measurement conditions. Despite considerable efforts to synthesize and purify ($R_{\text{nap}},S_{\text{py}}$)-1, especially at low temperature, it was not obtained.

To examine chiral transfer from the binaphthyl to the biaryl system, the conformations of (S_{nap})-4 and (R_{nap})-5 were also investigated. The X-ray crystal structure of (S_{nap})-4 confirms that the conformation of its biphenyl axis is S_{ph} and that of the bipyridyl axis in (R_{nap})-5 is R_{py} (Figures S3 and S4). In addition,

other geometrical features of 1, 4, and 5 were also similar. In this type of binaphthyl-biaryl cyclic dyad, the binaphthyl and any biaryl presumably twist in the same direction; that is, the (R)-binaphthyl moiety induces (R)-biaryl, whereas the (S)-binaphthyl moiety induces (S)-biaryl (care is needed concerning inversion of the label R or S merely according to the order of priority.)

We also observed the fluorescence properties of (R_{nap})-1. (R_{nap})-1 shows negligible fluorescence in common organic solvents such as tetrahydrofuran, 1,4-dioxane, chloroform, dichloromethane, dimethyl sulfoxide, acetonitrile, pyridine, and benzene, irrespective of the excitation wavelength ($\Phi_{\text{fl}} \leq 0.02$; this fluorescence is derived mainly from the binaphthyl moiety). However, it is interesting to note that ($R_{\text{nap}},R_{\text{py}}$)-1 exhibits fluorescence in the crystal state, which is unusual for a metal-free bipyridyl. This crystallization-induced emission enhancement (CIEE)¹⁶ behavior may be due to the influence of not only molecular packing but also the fixed bipyridyl structure with moderate θ_{py} .¹⁷ Compounds (S_{nap})-4 and (R_{nap})-5 show no CIEE characteristics. Figure 6 shows the FL spectrum of the

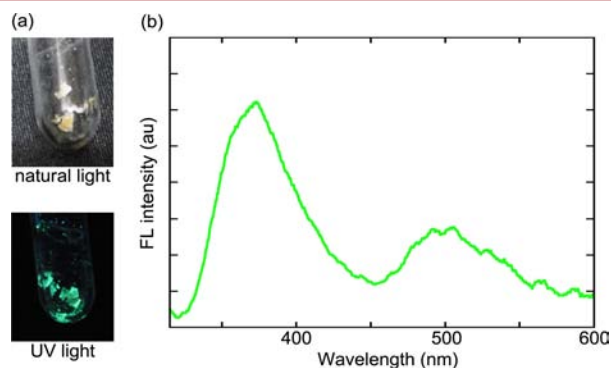


Figure 6. Fluorescence properties of the crystal of ($R_{\text{nap}},R_{\text{py}}$)-1· CHCl_3 . (a) Pictures of the crystal under natural and UV light (365 nm , rt). (b) Fluorescence spectrum of the crystal ($\lambda_{\text{ex}} = 300\text{ nm}$, rt).

crystal of ($R_{\text{nap}},R_{\text{py}}$)-1· CHCl_3 , which has a greenish-yellow emission ($\Phi_{\text{fl}} = 0.070$). The maximum and the local maximum λ_{em} values are 375 nm and around 500 nm , respectively. The former FL region is less visible to the human eye and is derived from the binaphthyl moiety,¹⁸ whereas the visible latter region is derived from the bipyridyl moiety.¹⁹ Other crystals exhibited rather similar emission spectra and quantum yields (Figures S13 and S14).

We anticipated that conformational and/or electronic changes upon protonation/deprotonation would lead to changes of chiroptical properties, at least to some degree. To investigate the switching of the chiroptical properties of ($R_{\text{nap}},R_{\text{py}}$)-1, we measured the specific optical rotation, $[\alpha]_{\text{D}}$, before and after protonation by adding trifluoroacetic acid (TFA) and deprotonation by titration with triethylamine (TEA) as a trial. The $[\alpha]_{\text{D}}$ value of ($R_{\text{nap}},R_{\text{py}}$)-1 in CH_3OH ($c = 0.10$) at 20°C is $+413$. In contrast, that of (R_{nap})-1· 2H^+ formed by titration of 2.2 equiv of TFA was changed to $+481$. Because the energy profile of θ_{py} of (R_{nap})-1· 2H^+ roughly agrees with that of (R_{nap})-1 (Figure S10), the $[\alpha]_{\text{D}}$ change should not be due to a major conformational change, but to protonation itself or a minor conformational change. Additional titration with 2.4 equiv of TEA restored the $[\alpha]_{\text{D}}$ value to $+409$. Thus, ($R_{\text{nap}},R_{\text{py}}$)-1 is a new prototype for a pH-activated chiroptical switch.

In summary, we synthesized compound **1**, in which axially chiral binaphthyl and bipyridyl were connected by short $-\text{CH}_2\text{O}-$ linkers, together with its analogues **4** and **5**. X-ray diffraction and VCD spectra confirmed the structure of the dyads in the solid state and in solution, respectively. Each binaphthyl induces a similar and unidirectional twist of the connected biaryls. This work shows that VCD has the potential to be a standard technique to determine the axial chirality of 2,2'-bipyridyl compounds. Further, the binaphthyl-biaryl system provides an easy route to construct any axially chiral biaryl. In crystals, (R_{nap}) -**1** possesses significant FL properties. Moreover, protonation/deprotonation alters the optical rotation of (R_{nap}) -**1**. We are currently investigating the circularly polarized luminescence (CPL) properties of **1** and preparing **1** metal complexes and their derivatives with specific conformations to further evaluate the (chir)optical properties and asymmetric catalytic functions.

■ ASSOCIATED CONTENT

📄 Supporting Information

The Supporting Information is available free of charge on the ACS Publications website at DOI: [10.1021/acs.orglett.5b02041](https://doi.org/10.1021/acs.orglett.5b02041).

Synthesis, spectra, and computational details (PDF)
 Crystallographic data for $(R_{\text{nap}}, R_{\text{py}})$ -**1**·CHCl₃ (CIF)
 Crystallographic data for $(R_{\text{nap}}, R_{\text{py}})$ -**1**·1/3H₂O (CIF)
 Crystallographic data for $(R_{\text{nap}}, R_{\text{py}})$ -**1**·1/2(MeOH)·H₂O (CIF)
 Crystallographic data for $(S_{\text{nap}}, S_{\text{ph}})$ -**4** (CIF)
 Crystallographic data for $(S_{\text{nap}}, S_{\text{py}})$ -**5** (CIF)

■ AUTHOR INFORMATION

Corresponding Authors

*E-mail: takaishi@okayama-u.ac.jp.

*E-mail: ayokoyama@st.seikei.ac.jp.

Present Address

#Graduate School of Natural Science and Technology, Okayama University, Tsushima, Okayama 700–8530, Japan

Notes

The authors declare no competing financial interest.

■ ACKNOWLEDGMENTS

We thank members of the molecular characterization team at RIKEN for the mass spectral measurements. The calculations were performed by using the RIKEN Integrated Cluster of Clusters (RICC) and HOKUSAI GreatWave (HOKUSAI-GW).

■ REFERENCES

- (1) Selected reviews for application of 2,2'-bipyridyl compounds: (a) Kaes, C.; Katz, A.; Hosseini, M. W. *Chem. Rev.* **2000**, *100*, 3553–3590. (b) Chelucci, G.; Thummel, R. P. *Chem. Rev.* **2002**, *102*, 3129–3170. (c) Maury, O.; Le Bozec, H. *Acc. Chem. Res.* **2005**, *38*, 691–704.
- (2) Selected examples of asymmetric reaction using 2,2'-bipyridyl compounds: (a) Lyle, M. P. A.; Draper, N. D.; Wilson, P. D. *Org. Biomol. Chem.* **2006**, *4*, 877–885. (b) Kobayashi, S.; Xu, P.; Endo, T.; Ueno, M.; Kitano, T. *Angew. Chem., Int. Ed.* **2012**, *51*, 12763–12766. (c) Kitano, T.; Xu, P.; Isshiki, S.; Zhu, L.; Kobayashi, S. *Chem. Commun.* **2014**, *50*, 9336–9339.
- (3) (a) Botteghi, C.; Schionato, A.; De Lucchi, D. *Synth. Commun.* **1991**, *21*, 1819–1823. (b) Shimada, T.; Kina, A.; Hayashi, T. *J. Org. Chem.* **2003**, *68*, 6329–6337. (c) Bouet, A.; Heller, B.; Papamicaël, C.; Dupas, G.; Oudeyer, S.; Marsais, F.; Levacher, V. *Org. Biomol. Chem.* **2007**, *5*, 1397–1404. (d) Durand, J.; Zangrando, E.; Carfagna, C.;

Milani, B. *Dalton Trans.* **2008**, 2171–2182. (e) Haberhauer, G. *Angew. Chem., Int. Ed.* **2008**, *47*, 3635–3638. (f) Chelucci, G.; Sanfilippo, C. *Tetrahedron: Asymmetry* **2010**, *21*, 1825–1829.

(4) (a) Takaishi, K.; Kawamoto, M.; Tsubaki, K.; Furuyama, T.; Muranaka, A.; Uchiyama, M. *Chem. - Eur. J.* **2011**, *17*, 1778–1782. (b) Takaishi, K.; Muranaka, A.; Kawamoto, M.; Uchiyama, M. *J. Org. Chem.* **2011**, *76*, 7623–7628. (c) Takaishi, K.; Muranaka, A.; Kawamoto, M.; Uchiyama, M. *Org. Lett.* **2012**, *14*, 276–279. (d) Takaishi, K.; Kawamoto, M.; Muranaka, A.; Uchiyama, M. *Org. Lett.* **2012**, *14*, 3252–3255.

(5) (a) Maigrot, N.; Mazaleyrat, J. P. *Synthesis* **1985**, 317–320. (b) Ooi, T.; Kameda, M.; Maruoka, K. *J. Am. Chem. Soc.* **2003**, *125*, 5139–5151.

(6) (a) Naumann, C.; Langhals, H. *Synthesis* **1990**, 279–281. (b) Reynal, A.; Etxebarria, J.; Nieto, N.; Serres, S.; Palomares, E.; Vidal-Ferran, A. *Eur. J. Inorg. Chem.* **2010**, *2010*, 1360–1365.

(7) Tiecco, M.; Testaferri, L.; Tingoli, M.; Chianelli, D.; Montanucci, M. *Synthesis* **1984**, 736–738.

(8) All calculations were performed using Gaussian09, revision D.01. Frisch, M. J., et al. Gaussian, Inc., Wallingford CT, 2013. See [Supporting Information](#) for full reference.

(9) Computational prediction of the transition state structure for the isomerization of (R_{nap}) -**1** has been tried by QST2 and QST3 methods, but the transition state was not convergent.

(10) Jaime, C.; Font, J. *J. Org. Chem.* **1990**, *55*, 2637–2644.

(11) Rebeck, J. J.; Costello, T.; Wattlely, R. *J. Am. Chem. Soc.* **1985**, *107*, 7487–7493.

(12) (a) Harada, N.; Nakanishi, K. *Acc. Chem. Res.* **1972**, *5*, 257–263. (b) Di Bari, L.; Pescitelli, G.; Salvadori, P. *J. Am. Chem. Soc.* **1999**, *121*, 7998–8004. (c) Di Bari, L.; Pescitelli, G.; Marchetti, F.; Salvadori, P. *J. Am. Chem. Soc.* **2000**, *122*, 6395–6398.

(13) (a) Stephens, P. J.; Devin, F. J.; Cheeseman, J. R. *VCD Spectroscopy for Organic Chemists*; CRC Press: Boca Raton, FL, 2012. (b) Nafie, L. A. *Vibrational Optical Activity: Principles and Applications*; J. Wiley & Sons: Chichester, U.K., 2011.

(14) (a) Strucl, J. S.; Walter, J. L. *Spectrochim. Acta, Part A* **1971**, *27*, 209–221. (b) Castellucci, E.; Angeloni, L.; Neto, N.; Sbrana, G. *Chem. Phys.* **1979**, *43*, 365–373. (c) Neto, N.; Muniz-Miranda, M.; Angeloni, L.; Castellucci, E. *Spectrochim. Acta, Part A* **1983**, *39*, 97–106. (d) Brolo, A. G.; Jiang, Z.; Irish, D. E. *J. Electroanal. Chem.* **2003**, *547*, 163–172. (e) Wu, T.; Zhang, X. P.; You, X. Z. *RSC Adv.* **2013**, *3*, 26047–26051.

(15) Taniguchi and Monde reported versatile applications of VCD for dicarbonyl compounds: Taniguchi, T.; Monde, K. *J. Am. Chem. Soc.* **2012**, *134*, 3695–3698.

(16) Selected reports on the CIEE of metal-free compounds: (a) Shimizu, M.; Takeda, Y.; Higashi, M.; Hiyama, T. *Angew. Chem., Int. Ed.* **2009**, *48*, 3653–3656. (b) Imoto, M.; Ikeda, H.; Fujii, T.; Taniguchi, H.; Tamaki, A.; Takeda, M.; Mizuno, K. *Org. Lett.* **2010**, *12*, 1940–1943. (c) Luo, X.; Li, J.; Li, C.; Heng, L.; Dong, Y. Q.; Liu, Z.; Bo, Z.; Tang, B. Z. *Adv. Mater.* **2011**, *23*, 3261–3265. (d) Zhu, Q.; Huang, L.; Chen, Z.; Zheng, S.; Lv, L.; Zhu, Z.; Cao, D.; Jiang, H.; Liu, S. *Chem. - Eur. J.* **2013**, *19*, 1268–1280. (e) Galer, P.; Korošec, R. C.; Vidmar, M.; Šket, B. *J. Am. Chem. Soc.* **2014**, *136*, 7383–7394. (f) Yoshii, R.; Hirose, A.; Tanaka, K.; Chujo, Y. *J. Am. Chem. Soc.* **2014**, *136*, 18131–18139.

(17) Partial solid-state assembled structures are shown in Figure S5 in the [Supporting Information](#). Apparent π -stacking is not observed, and molecules of (R_{nap}) -**1** seem to be separated from each other by solvent molecules.

(18) Fluorescence of simple binaphthyl compounds in the solid state has been reported: Takaishi, K.; Kawamoto, M.; Tsubaki, K. *Org. Lett.* **2010**, *12*, 1832–1835.

(19) Fluorescence of metal-free bipyridyl compounds in the solid state has been reported: (a) Sreejith, S.; Divya, K. P.; Ajayaghosh, A. *Chem. Commun.* **2008**, 2903–2905. (b) Sarma, M.; Chatterjee, T.; Ghanta, S.; Das, S. K. *J. Org. Chem.* **2012**, *77*, 432–444.